VTT Technical Research Centre of Finland

On the hydrodynamic design of podded propulsors for fast commercial vessels

Sánchez-Caja, Antonio; Pylkkänen, Jaakko V.

Published in:
Proceedings of 1st International Conference on Technological Advances in Podded Propulsion

Published: 01/01/2004

Document Version
Publisher's final version

ON THE HYDRODYNAMIC DESIGN OF PODDED PROPULSORS FOR FAST COMMERCIAL VESSELS

Antonio Sánchez-Caja, VTT Industrial Systems, Finland
Jaakko V. Pylkkänen, VTT Industrial Systems, Finland

Within the European Union FASTPOD project the application of electric drive podded propulsors to high-speed commercial vessels is being studied. In particular a Ropax and a cargo ship have been selected as candidates for speeds of 35-38 knots. For such high speeds the hydrodynamic design of the propeller with its housing is critical due to the danger of cavitation on both propeller blades and supporting strut. This paper deals with the optimization process of the propeller housing using RANS solver FINFLO. A non-symmetric strut is designed in order to delay cavitation inception keeping at the same time low drag and low lateral forces on the strut. A remarkable reduction of low-pressure areas is observed on the strut surfaces for a tailor-made design as compared to a conventional symmetric strut. Several pod configurations are also analyzed.

1. Introduction

Over the last decade RANS tools have been increasingly applied to the hydrodynamic design of propulsors. Primarily RANS equation methods are analysis tools as opposed to design ones. However, they can be used in an iterative way for design exercises provided that a geometry close to the final target be defined by other means, for example by the designer experience, by design constraints or for exploring new concepts by simpler calculation methods as those based on potential theory.

When facing the problem of propulsor optimization, the designer must not forget that his aim is to achieve a geometry that works properly at full scale. Usually during the design phase experiments at model scale are carried out and provisions are made to account for differences of flow regimes at model and full scale. The extrapolation of model scale results to full scale should be made very carefully specially in the case of complex propulsors, and in particular of podded propulsors.

Podded propulsors consist of several parts that can behave in very different ways from the standpoint of scaling viscosity effects (Sánchez-Caja et al., 2003). Some parts are lifting devices such as struts or potential fins for which reduction of trailing edge separation from model to full scale can mean strong increases of their lifting capabilities and consequently, noticeable reductions in pressure drag. Such reductions would not be significant in the case of lifting bodies with non-separated flow in model scale, where the reductions would be due only to drops in frictional drag. Other parts are non-lifting bodies that can behave also very differently at model and full scale depending on their capability to reduce areas of flow separation as the Reynolds number increases.

Traditionally the optimization process of a propulsor has been made within the assumption that a propeller that is optimum at model scale would also be optimum or almost optimum at full scale. Such assumption may be more in question for the case of podded propulsors. However, there are macroscopic effects at full scale that can be captured with model scale experiments or calculations. In this paper we are focusing mainly on such effects, leaving for a future paper issues related to the extrapolation to full scale.

When applying podded propulsors to fast commercial ships the designer encounters new challenges not present in low speed applications. In particular cavitation both on the propeller blades and on the housing is difficult to avoid and therefore problems of noise, erosion and decreased efficiency may arise. A way of reducing the danger of cavitation may be to distribute the propulsion loading among several propellers and to make a careful choice of the housing geometry. This has been the approach chosen in the FASTPOD project. In this paper the main focus is the housing optimization of the Ropax vessel.

2. RANS code as design tool

At the first stages of the design a fast tool of hydrodynamic analysis is desired that can take into account the main viscous phenomena undergone by alternative geometries of the propulsor unit. At the same time it should provide information on the pressure distribution over the surfaces of the housing in order to control the inception of cavitation. RANS solvers can be used here provided that the grid generation process be minimized and that the calculation time be also confined within reasonable limits.

At VTT the grid generation process has been automatized by using an in-house developed computer program, which allows to build grids for alternative housings very rapidly. The program can be also applied to modifying propeller blades.

The calculation time has been controlled by making simplifications in the representation of the propeller and by using grids not to large although with good resolution at the boundary layer level. Good resolution close to the geometric boundaries of the housing was required since our solver does not use wall functions. It is known that in principle, extending the solution to the wall makes more accurate the prediction of flow detachment at the cost of somewhat larger grid size.

In the first stages of the design, calculations were made for housings subjected to an inflow defined from the conditions in the wake of the propeller at a distance corresponding to the location of the maximum thickness of the strut. For these calculations no interaction effects between the strut and the propeller were considered. In order to implement properly the inlet boundary condition on the inflow a cylinder was placed in front of the propeller plane. The flow was allowed to slip over the cylinder so as to prevent an non-physical growth of the boundary layer.

Concerning the computational size grids of about 3.4 millions cells were built for alternative geometries tested. However, the preliminary calculations were made with coarser grids of about 0.43 million cells corresponding to a coarse level of the original grids, in which every other grid line was removed. The fine grids were used only at the final stage and only for the best hydrodynamic configurations to ascertain the right choice of the final geometry. Figure 1 illustrates a coarse grid. It corresponds to the grid used for the analysis of one of the non-symmetric strut-pod configuration about which we will speak later. High resolution near the strut surfaces in the propeller wake is employed in order to accurately capture details of the flow on the strut. All the figures presented in this paper correspond to calculations with the coarse grids unless otherwise specified.

The FINFLO solver has been used in this work for the analysis of the different geometrical configurations.

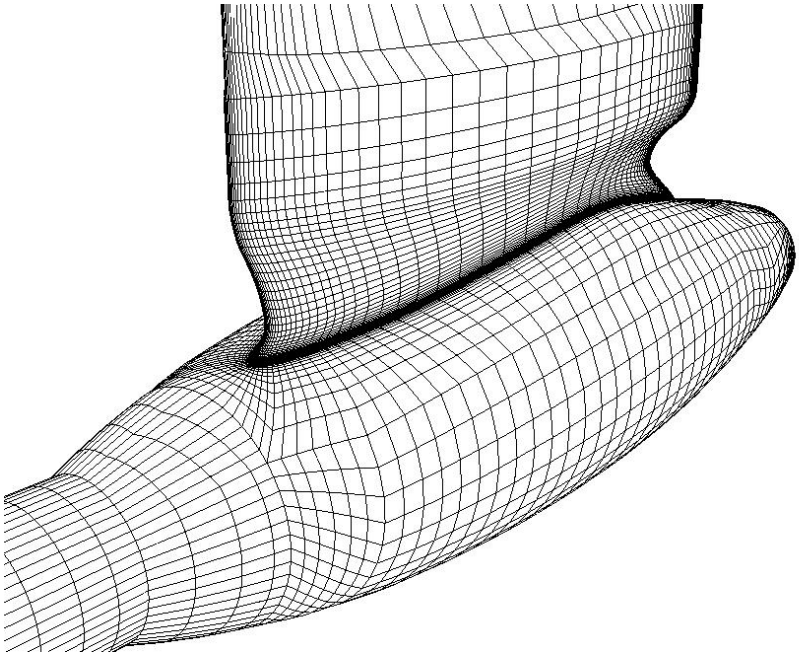

Figure 1. Illustration of a coarse grid used for the first stages of the design. The strut is asymmetric. High resolution was confined to the portion of the strut located in the propeller wake.

3. Numerical method

The flow simulation in FINFLO is based on the solution of the RANS equations by the pseudo-compressibility method. FINFLO solves the RANS equations by a finite volume method. The solution is extended to the wall and is based on approximately factorized time-integration with local time-stepping. The code uses either Roe's flux-difference splitting or Van Leer's flux-vector splitting. A multigrid method is used for the acceleration of convergence. Solutions in coarse grid levels are used as starting point for the calculation in order to accelerate convergence. A detailed description of the numerical method including discretization of the governing equations, solution algorithm, etc. can be found in Sanchez-Caja et al. (1999 and 2000). Chien's low Reynolds number k-epsilon model has been used in the calculation.

As an example, Figures 2 and 3 illustrate the convergence history of the overall drag. They correspond to computations on the coarse and fine grids respectively for the final geometry of the housing. Using 6 processors of moderate capacity (700 MHz Intel Xeon) in Windows environment a couple of geometries could be analyzed per day. This number could be multiplied by more than 4-5 if state-of-art processors were used instead. From the figures it can be seen that the size of the coarse grid is far from the zone of grid-independent results.

4. Strut optimization

Some FASTPOD partners provided an initial geometry for the housing of the podded propulsor. The goal of VTT was to make it suitable for high-speed operation around 38 knots. The first RANS analysis revealed low-pressure areas below the cavitation number on both sides of the strut near the location of maximum thickness. As expected the larger low-pressure area was on the suction side of the strut. Figures 4 and 6 show the pressure distributions on the pressure and suction side of the

strut, respectively for the coarse grids. The lowest color approximately represents areas of pressure below the cavitation number.

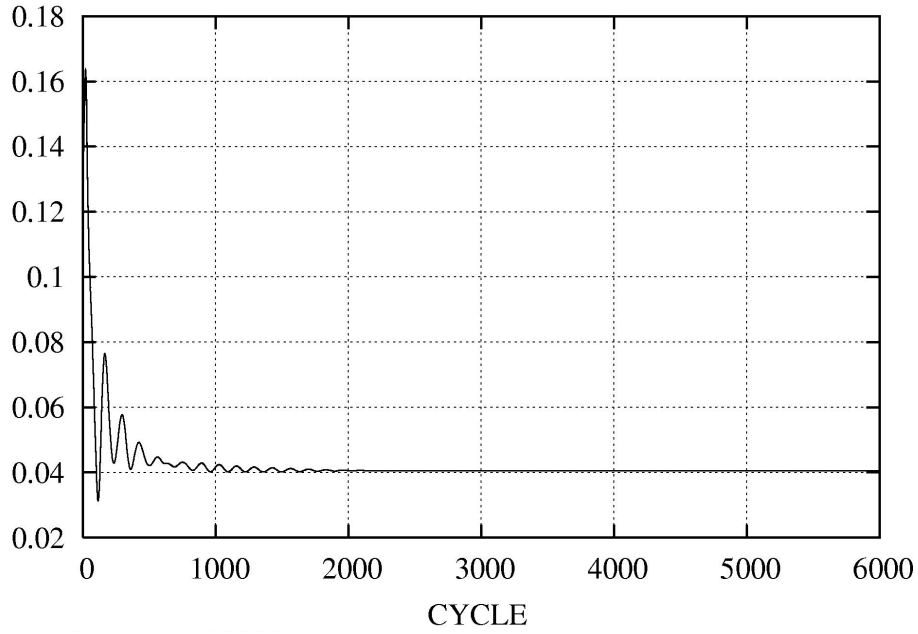

Figure 2. Example of convergence history for overall drag of a coarse grid.

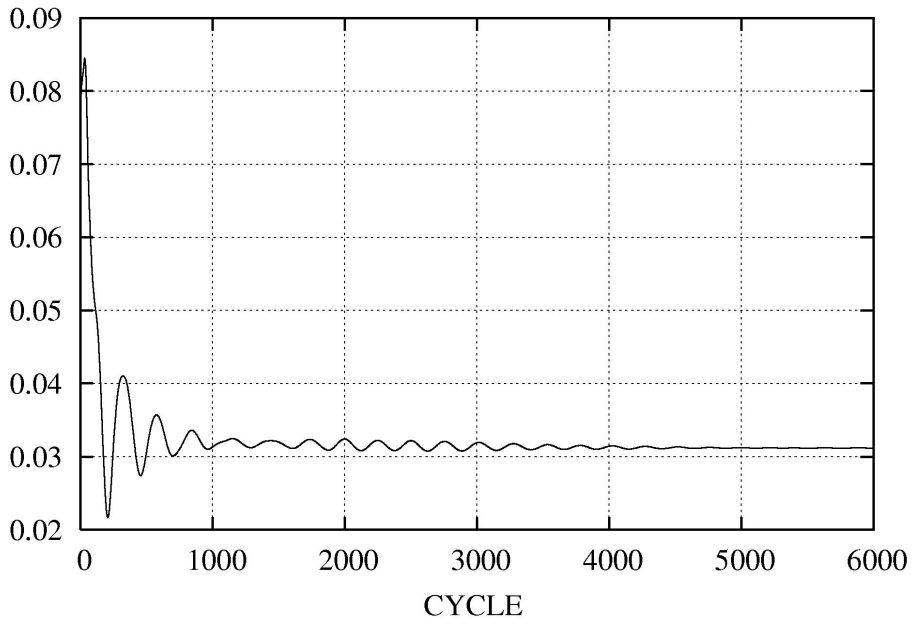

Figure 3. Example of convergence history for overall drag of a fine grid.

In order to get rid of low-pressure areas on the strut, the thickness distribution was redefined and it was decided that the strut should become non-symmetric. Our goal was to unload the strut keeping at the same time low levels of viscous drag. Several shapes were investigated and the geometry

shown in Figures 5 and 7 was selected. From the figures it can be seen that the low-pressure areas below the cavitation number have completely disappeared for the modified strut. Moreover there is still cavitation margin, which can be used for either increasing the speed of the vessel or allowing wider variations in the attack angle of the inflow to the strut. Such variations can be caused for example by the unsteadiness of the propeller wake or by ship maneuvering.

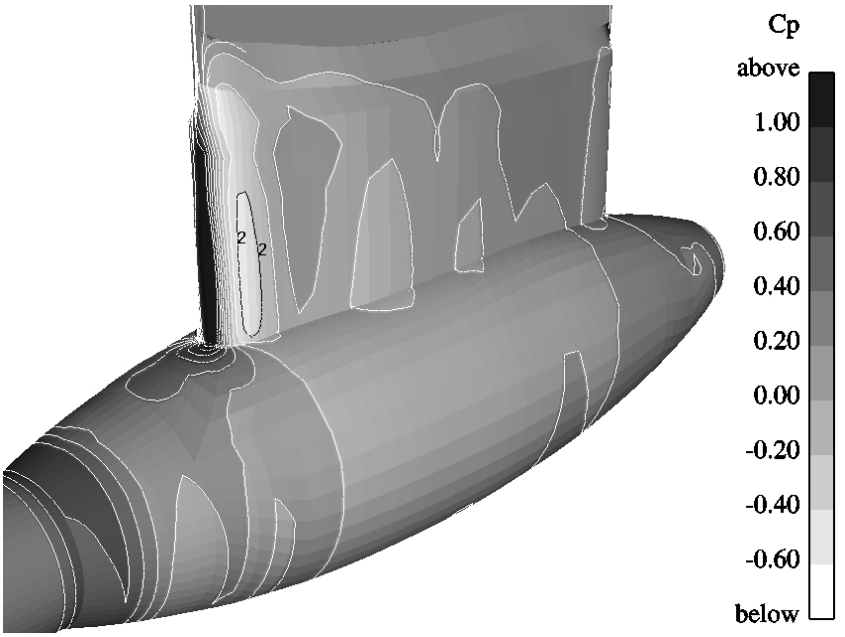

Figure 4. Pressure distribution on the initial version of the housing. Strut pressure side. The white color surrounded by contour labeled 2 shows pressure below the cavitation number.

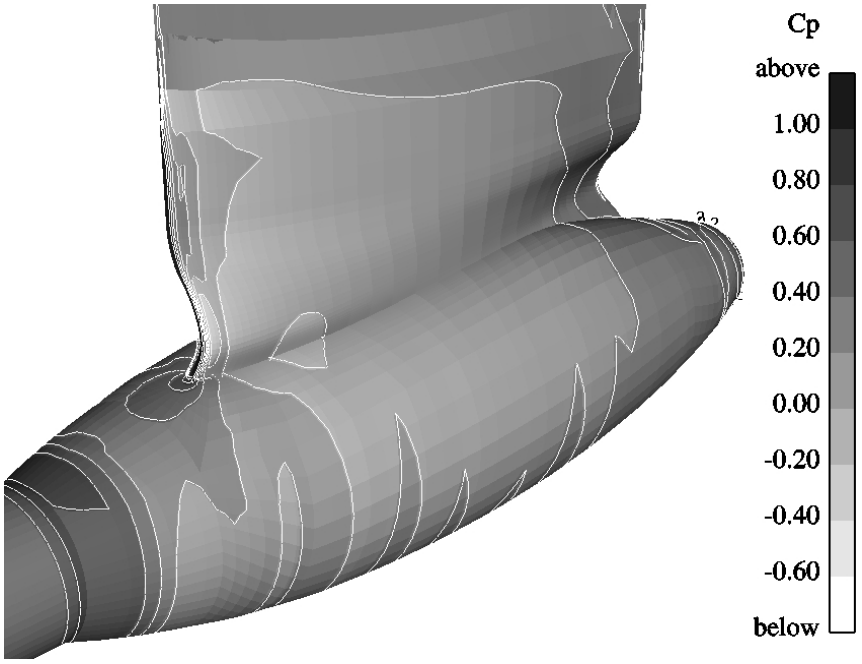

Figure 5. Pressure distribution on the asymmetric housing. Strut pressure side. The pressure falls no more within the lowest level in the scale.

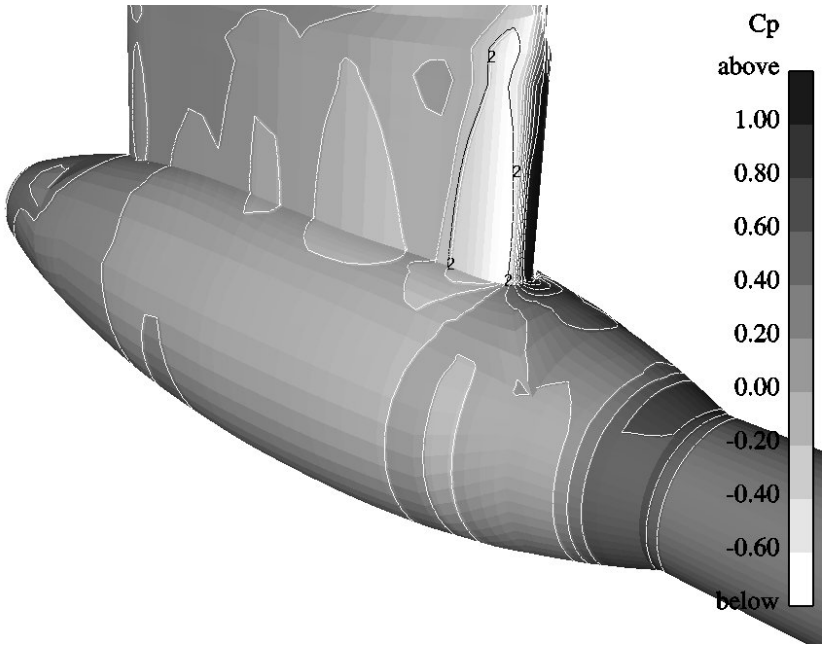

Figure 6. Pressure distribution on the initial version of the housing. Strut suction side. The white color surrounded by contour labeled 2 shows pressure below the cavitation number.

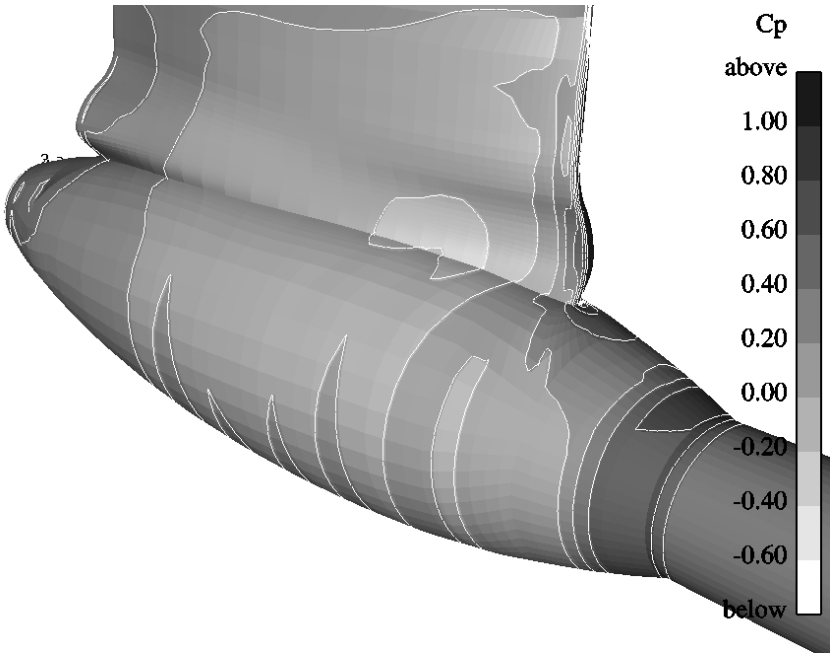

Figure 7. Pressure distribution on the asymmetric housing. Strut suction side. The pressure falls no more within the lowest level in the scale.

5. Pod optimization

After the initial calculations defining the strut shape, other work packages of FASTPOD revised the design constraints concerning the motor main dimensions. This revision mainly affected the minimum pod length which was increased. At the same time the minimum value of the strut length

was significantly reduced. Other constraints came from the fact that two out of the four pod units are designed as rotatable units, which imposes additional limitations on the maximum length of the pods.

A new set of computations was made focusing this time mainly on the pod shape. Several pod lengths were studied and alternative shapes for the pod aft part were numerically tested. An initial pod shape with a large blunt end (shown in Figure 8) was discarded due to low-pressure areas and high drag. A second pod with very smooth recovery of pressure at the aft end leading to almost non-separated flow at model scale and relatively long was found with less drag than the first one. A third pod with a small blunt aft end, but substantially shorter than the second one, was found to have slightly more drag than the second one. The reason was that the penalty due to the small separation area caused by the small blunt aft end was of the same order of magnitude than that due to the increased wetted area of the longer pod. This pod is shown in Figure 9. However, limitations on the pod length made us search for a solution close to the short pod. Finally a short pod with a cap of revolution at the aft end was selected. A small area of flow separation in model scale was allowed, which is expected to be reduced in full scale. This pod is shown in Figure 10.

Table I. Figures of merit for different pod versions. Coarse grid. Lower values mean better shape

Initial pod	100
smooth, long pod	74
short pod	76
final pod	71

Table II. Figures of merit for different pod versions. Fine grid. Lower values mean better shapes

short pod	100
final pod	97

The calculations were made with the 0.43 million cell grid for all the geometries tested and with the 3.4 million grids only for those with lower drags. As the coarse grid sizes are far from a numerically converged solution the drag coefficients obtained can be considered as a figure of merit for qualitative comparison. Table I shows such figures expressed as percentages of the initial pod drag for the four versions. Table II shows a similar comparison using the finer grids for the third and fourth pods. The differences are smaller for the fine grids (3% versus 7% of the coarse grid).

For the first pod (Fig. 8) the low-pressure peak on the circular rear surface results in pressure drag and probably cavitation. For the third pod (Fig. 9) the low-pressure peak is significantly smaller. Figure 10 shows the streamlines on the aft end of the final pod. Increasing the pod length can further reduce the area of flow separation and consequently the drag at model scale.

6. Conclusion

The application of RANS solver FINFLO to the hydrodynamic design of podded propulsors for high-speed operation has been described. Even though RANS solvers are analysis tools as opposed to design ones, they can be used iteratively for design purposes. The right choice of the

computational grid together with the computational model make it possible to test alternative geometries in relative short time.

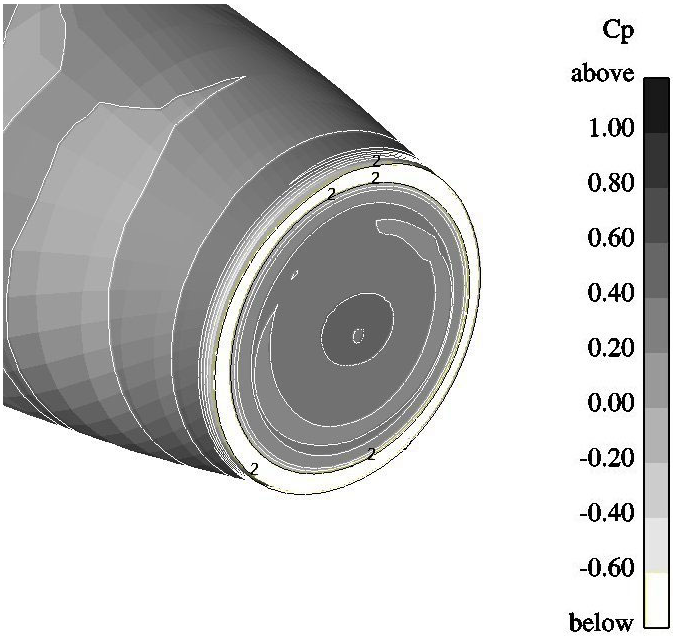

Figure 8. Pressure distribution on a pod with a large blunt aft end (initial shape). The white color surrounded by contour labeled 2 shows pressure below the cavitation number.

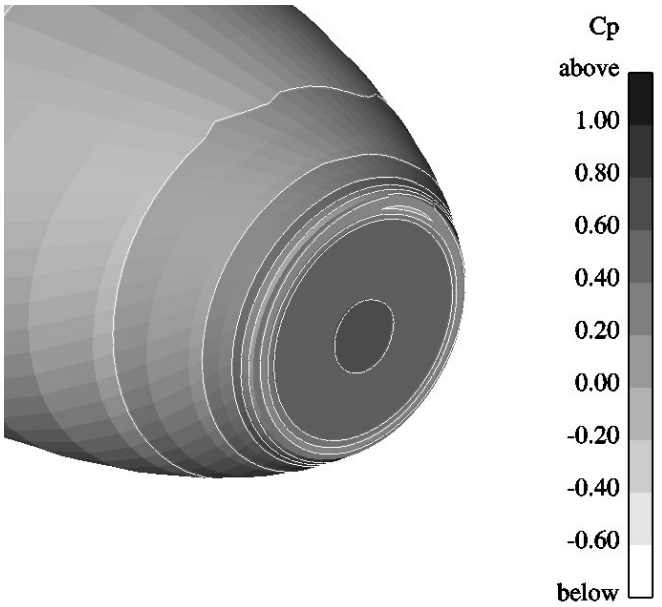

Figure 9. Pressure distribution on a pod with a small blunt aft end.

For high speeds the design of the propeller with its housing is critical due to the danger of cavitation on both propeller blades and supporting strut. A non-symmetric strut is designed in order to delay cavitation inception keeping at the same time low drag and low lateral forces on the strut. A remarkable reduction of low-pressure areas is observed on the strut surfaces for a tailor-made

design as compared to a conventional symmetric strut. Several pod configurations have been also analyzed. Their hydrodynamic merit is evaluated on the basis of RANS results.

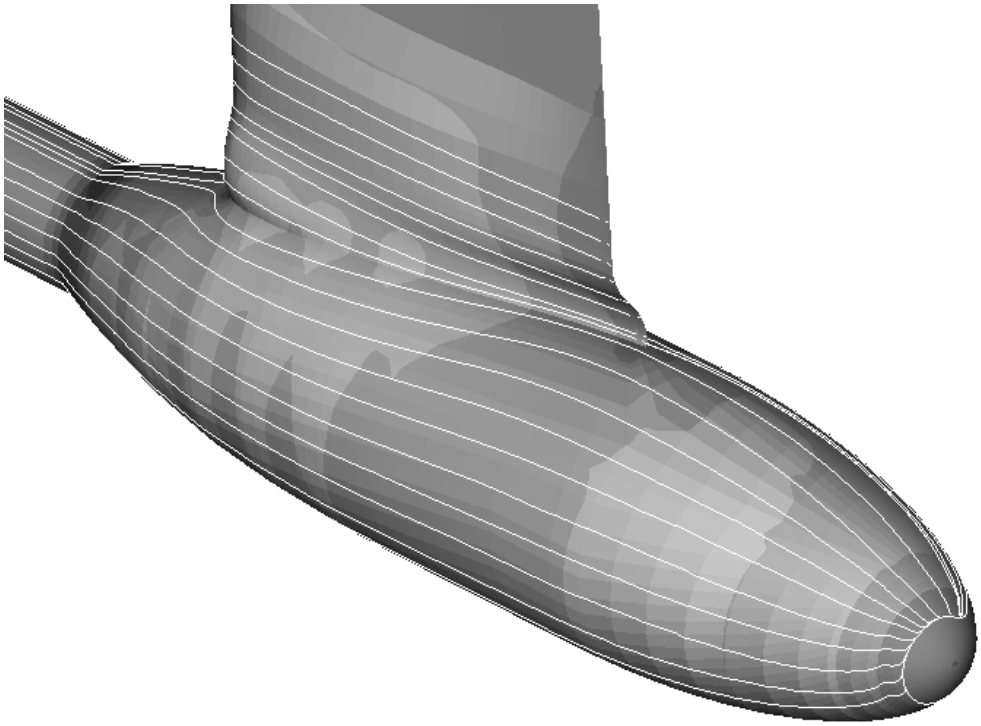

Figure 10. Streamlines on the aft end of the final pod.

Acknowledgements

This work has been made within the European Union FASTPOD project. The authors wish to thank the partners in the FASTPOD project.

References

1. Sanchez-Caja, Antonio; Ory, Emmanuel; Salminen, Esa; Pylkkänen, Jaakko & Siikonen, Timo. "Simulation of Incompressible Viscous Flow Around a Tractor Thruster in Model and Full Scale". The 8th International Conference on Numerical Ship Hydrodynamics, Busan (Korea), September 22-25, 2003.

2. Sánchez-Caja, A., Rautaheimo, P., Salminen, E., and Siikonen, T., "Computation of the Incompressible Viscous Flow around a Tractor Thruster Using a Sliding Mesh Technique", 7th International Conference in Numerical Ship Hydrodynamics, Nantes (France), 1999.

3. Sánchez-Caja, A., Rautaheimo, P. and Siikonen, T., "Simulation of Incompressible Viscous Flow Around a Ducted Propeller Using a RANS Equation Solver", 23rd Symposium on Naval Hydrodynamics, Val de Reuil (France), 2000.